DOI 10.1007/s11595-016-1389-5

Fabrication of Micro/Nano-textured Titanium Alloy Implant Surface and Its Influence on Hydroxyapatite Coatings

ZHANG Rui[1], WAN Yi[1*], AI Xing[1], MEN Bo[1], WANG Teng[1], LIU Zhanqiang[1], ZHANG Dong[2]

(1. Key Laboratory of High Effciency and Clean Mechanical Manufacture, Ministry of Education, School of Mechanical Engineering, Shandong University, Shandong 250061, China; 2. Qilu Hospital, Shandong University, Shandong 250002, China)

Abstract: We put forward a protocol combining laser treatment and acid etching to obtain multiscale micro/nano-texture surfaces of titanium alloy implant. Firstly, the operational parameters of the laser were optimized to obtain an optimum current. Secondly, the laser with the optimum operational parameters was used to fabricate micro pits. Thirdly, multiple acid etching was used to clean the clinkers of micro pits and generate submicron and nanoscale structures. Finally, the bioactivity of the samples was measured in a simulated body fluid. The results showed that the micropits with a diameter of 150 μm and depth of 50 μm were built successfully with the optimized working current of 13 A. In addition, submicron and nanoscale structures, with 0.5-2 μm microgrooves and 10-20 nm nanopits, were superimposed on micro pits surface by multiple acid etching. There was thick and dense HA coating only observed on the multiscale micro/nano-textured surface compared with polished and micro-textured surface. This indicated that the multiscale micro/nano-texture surface showed better ability toward HA formation, which increased the bioactivity of implants.

Key words: titanium alloy implant; laser treatment; acid etching; bioactivity; micro/nano-textures

1 Introduction

The healing process, which follows the surgical implantation of dental and bone fixtures in the human body, determines the final outcome of a surgery. Rejection reactions appear after implantation because of poor bio and mechanical compatibilities of traditional implants. Sometimes, the implants may be ejected from the body. Therefore, improving the contact between the implant and tissue is a key factor influencing the success of the surgery[1]. Among the many factors influencing osseointegration, surface topography has been most widely studied[2]. Compared to the smooth and machined surfaces, implants with micro/nano-textures have shown higher success rates[3]. In vitro and in vivo studies have shown the advantage of micro/nano-textures, which in addition to enhancing the cell growth, cell adhesion, cell migration, and proliferation, also improved the bone deposition and contact between the bone and implant[4-6]. In addition, some studies have shown that implants with micro-nano-textured surfaces possess stronger interfacial bonding strengths[7], increasing the stability of the implants in the body. Currently, the main processing methods used on implant surfaces are abrasive blasting[8], photolithography[9], titanium plasma spraying[10,11] and chemical treatment[12-14], *etc*. Traditional chemical, physical, and mechanical methods can generate rough surfaces; however, these methods cannot be used to obtain a specific morphology in the specified area. We believe that laser treatments can overcome this limitation.

Laser treatment is a new method to generate three-dimensional features in the micro-nano scale, which can be used to process complex surface topographies[15]. Some studies have proven that lasers can be used to generate microgrooves and micro pits[16-19]. Kurella and Dahotre described the advantages of laser machining on the microstructure. For instance, the laser can remove material quickly, cleanly, selectivity, and generate complex microstructures on the surfaces, when a single wavelength of short pulses is used[20].

(Received: Oct. 13, 2015; Accepted: Nov. 28, 2015)

ZHANG Rui (张蕊): Ph D; E-mail: sduzhangrui@gmail,com

* Corresponding author: WAN Yi(万熠): Assoc. Prof.; E-mail: wanyi@sdu.edu.cn

Funded by the National Natural Science Foundation of China (51175306 and 51575320), the Tai Shan Scholar Foundation (TS20130922), and the Fundamental Research Funds for the Central Universities (2014JC020)

In this paper, we reported the first study of bioactive surface micro/nano-textures on the titanium alloy surface produced by a combination of laser treatment and acid etching. First, the laser machining parameters were optimized and then, micro pits were produced on the surface using the laser. The laser clinkers were cleaned and nanostructures were generated on the micro pits by acid etching. Bio-mineralisation testing was carried out to investigate the bioactivity of the samples with different surface structures. The surface morphology, structure, and components of the samples were studied by various surface analytical techniques.

2 Experimental

2.1 Materials and pre-treatment

Titanium alloy (Ti6Al4V) flat plates with dimensions of 10 mm × 10 mm × 1.5 mm were used in the experiments. The samples were polished by mechanical grinding and polishing, and further cleaned with acetone and water.

2.2 Optimization of the laser parameters

The sample surface was fabricated using an yttrium aluminium garnet (YAG) laser with a wavelength of 1064 nm and a spot diameter of 30μm. The electric current is one of the main influencing factors and the machining precision is controlled by changing power and energy. The samples were fabricated by laser machining using the single factor analysis method with different currents (I = 10, 11, 11.3, 11.5, 11.8, 12, 12.5, 13, 14, and 15 A). The optimized parameters were used to generate micro pits on the surface of the titanium alloy.

2.3 Multiple acid etching

Multiple acid etching was used to clean the laser clinkers and generate the submicron and nanoscale structures. The samples were first treated with a solution containing 0.09 mol/L HNO_3 and 0.11 mol/L HF at room temperature for 10 min. The samples were then treated with a solution containing 4.5 mol/L H_2SO_4 and 2.9 mol/L HCl at 80 ℃ for 25 min and subsequently, quickly cleaned with water. Then, the samples were treated with a solution of 98% H_2SO_4 and 30% H_2O_2 in a volume ratio of 1:1 at room temperature for 90 min. Finally, the samples were washed with distilled water.

2.4 Surface characterization and analysis

The surface morphology of the samples machined by the laser was analysed with a scanning electron microscope (SEM) and digital microscope. The surface elemental composition was determined by energy dispersive spectrometry (EDS).

2.5 Bioactivity estimation

The bioactivity of the samples was examined in a simulated body fluid (SBF) using Kokubo's recipe[21]. The samples were divided into three groups: polished (P), micro-nano-textured (MN), and micro pits (M). The samples belonging to the three groups were immersed in 30 mL of SBF in an Eppendorf tube and the pH value was adjusted to 7.4 at 37 ℃. After soaking in the SBF for 15 days, the samples were gently washed with distilled water and dried in air.

3 Results and discussion

3.1 Laser treatment and parameter optimization

The microstructures obtained on the titanium alloy surface after the laser treatment are clearly observed in Fig.1. Figs.1(a)-1(d) show the changes in the surface topography obtained using different laser electric currents. Colour changes occurred on the surface only when the current was 10 A (Fig.1(a)). With increasing current (11A-13A), the material removal and depth of the micro pits increased (Figs.1(b)-1(d)).

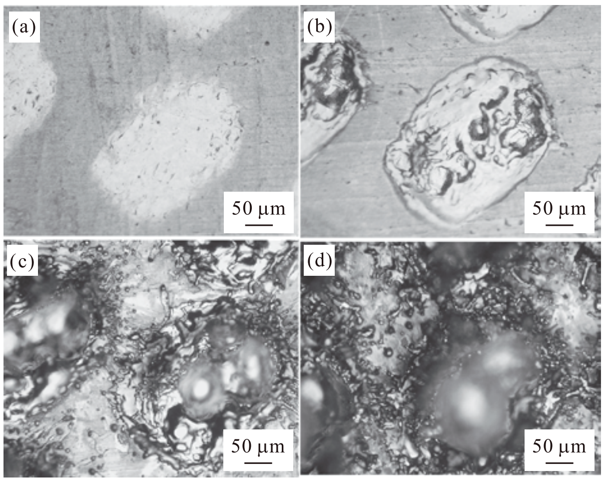

Fig.1 Digital images of Ti6Al4V surfaces obtained with different laser currents of (a) 10 A, (b) 11 A, (c) 12 A, and (d) 13 A

As the heat affected zone diffused into the sample, a deeper weld crater appeared. Because the thermal conductivity of Ti6Al4V is low, with increasing energy, the weld crater absorbs a significant amount of heat, although this heat is dissipated slowly. Hence, the weld crater temperature increased sharply to reach the boiling point of the material. Then, the material began to degenerate into a gaseous powder and generated a plasma. Subsequently, the boiling splash of material began to appear on the surface and micro pits with good morphology were generated, which was accompanied by ablation of the surface. After the laser treatment was ceased, recrystallization occurred on the surface and the microstructure also changed significantly, as shown in Figs.1(c) and 1(d). The relationship between the depth of the micro pits and current is shown in Fig.2.

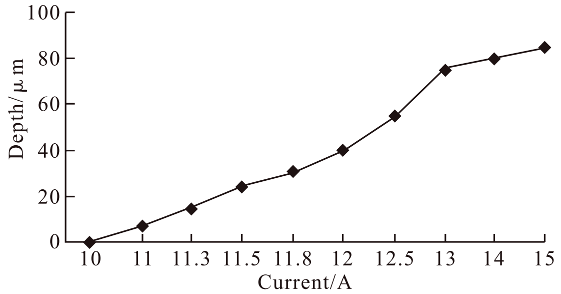

Fig.2 Variation of the micro pits depth with current

As shown in Fig.2, the micro pit depth increased with increasing current. However, when the current was greater than 13A, the depth increase slowed down. This can be attributed to two factors. First, the low heat conductivity coefficient generates a large amount of energy, which gathers in the weld crater and is not conducted to the deeper portions of the material. In addition, the small and focused processing area leads to the formation of a powder and the plasma generated by the prior pulse cannot be discharged from the pits before the next pulse arrives. This leads to cinder remains in the micro pits. Also, excess energy accumulation causes serious burn damages and destroys the performance of the material. Hence, the current value should not be excessively large. Considering the morphology and depth of the micro pits and the influence of energy on the material, we think 13 A is the optimum current.

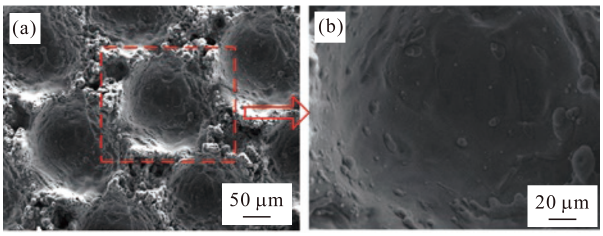

Fig.3 SEM images of Ti6Al4V surfaces after laser treatment

Fig.3 shows the characteristics of the micro pits produced by using the optimized laser parameters. On the inner surface and the edges of the pits, laser clinkers were distributed randomly. The diameter of the laser clinker ranged widely from 1 to 10 μm.

3.2 Fabrication of micro-nanostructures

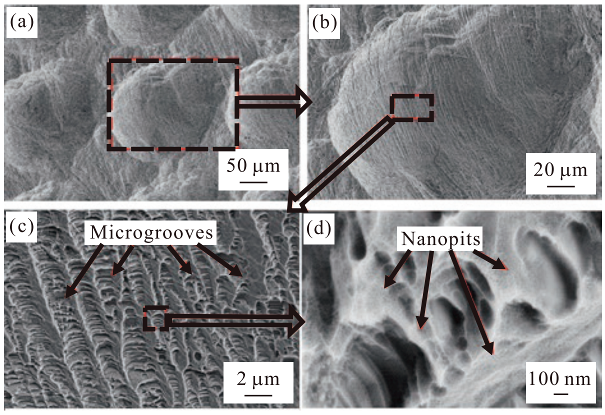

Fig.4 SEM images of the Ti6Al4V surfaces after multiple acid etching

Multiple acid etching was used to clean the clinker and generate submicron and nanoscale structures. Fig.4 shows the SEM images of the surface after laser processing and acid etching. As shown in Figs.4(a) and 4(b), the diameter of the micro pits array is about 150 μm and the separation is 20 μm. The depth of the micro pits, as examined by a digital microscope, was about 50 μm. The clinkers were cleared and microstructures consisting of rectangular grooves and ridges were produced in the titanium alloy (Fig.4(c)). The width of the grooves and ridges varied between 0.5 μm and 2 μm. As shown in Fig.4(d), a cluster of multiscale nanopits with diameters in the range of 10-20 nm were distributed on the micro pits.

Micron topography is conducive to early implant osseointegration[22,23]. Nano and submicron topography can directly regulate the cellular response to the material[24,25]. The micro/nano-textures are considered as surface modifications, which can improve the bioactivity of the titanium implant. These structures have been studied by some researchers both in vitro and in vivo[26]. It has previously been demonstrated that micro/nano-textures have an effect on bone formation, accelerating the regeneration of bone tissue and improving the mechanical binding force[27]. In the present study, the micro pits with diameter of 150 μm and the depth of 50 μm were created by laser processing. The submicron and nanoscale structures with 0.5-2 μm microgrooves and 10-20 nm nanopits were distributed on the micro pits surfaces. This type of multiscale micro/nano-texture features clearly show the potential to improve the mechanical and biocompatibilities of the material.

Figs.5(a) and 5(b) show the EDS profiles of the surface before and after acid etching. Carbon and oxygen were additional elements found on the surface after laser machining. After acid etching, C was removed completely, as shown in Fig.5(b).

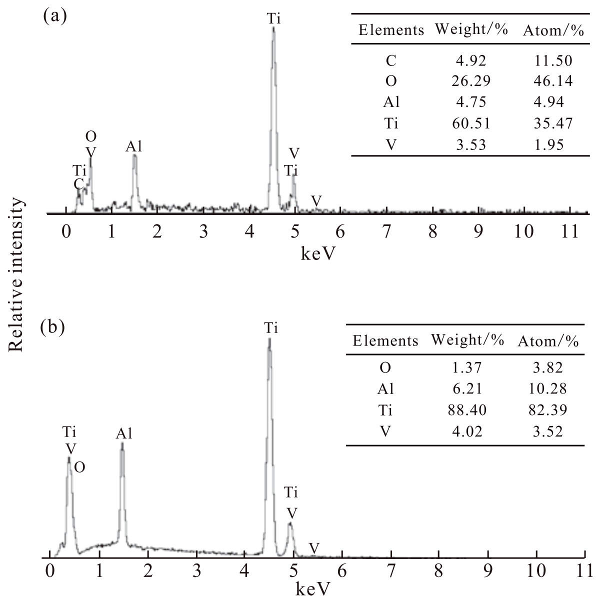

(a)

Elements	Weight/%	Atom/%
C	4.92	11.50
O	26.29	46.14
Al	4.75	4.94
Ti	60.51	35.47
V	3.53	1.95

(b)

Elements	Weight/%	Atom/%
O	1.37	3.82
Al	6.21	10.28
Ti	88.40	82.39
V	4.02	3.52

Fig.5 EDS profiles of the Ti6Al4V surfaces after (a) laser treatment and (b) acid etching

Because these clinkers have a weak adhesion with the material, their dislodgement from the implant after surgery leads to seriously toxic side-effects, such as cell toxicity, irritation, sensitization, and carcinogenicity[28]. Therefore, clinkers must be cleared to ensure the safety of the implant. As shown in Fig.5(a), carbon and oxygen peaks could be clearly seen in the EDS profiles of the clinker. The carbon content was 4.92%, markedly higher than the normal content encountered in Ti6Al4V (< 0.08%). This can be attributed to the reaction of the molten Ti6Al4V with carbon dioxide, which generates pollutants containing carbon during the laser treatment. The increase in oxygen is because the high energy of the laser increased the internal energy of the titanium alloy, which activates titanium atoms, facilitating reaction with oxygen. Consequently, TiO_2, Ti_3O_5, Ti_2O, and TiO were generated on the surface.

As shown in Fig.4(a), all the clinkers were removed. In addition, the EDS analysis of the surface showed the absence of carbon and only a small amount of oxygen was present on the surface (Fig.5(b)). The contents of the other three elements Ti, Al, and V were in agreement with the substrate elements. The elemental analyses obtained from the EDS profiles indicate the absence of clinker pollutants on the surface. The presence of a small amount of oxygen on the surface can be explained by the reaction between Ti and H_2O_2. It has been reported that titanium could react with H_2O_2 to form titania gel[29]. Fabrication of a titania gel coating is considered to be a potential method to improve the bioactivity of titanium implants[30].

3.3 Bioactivity analysis

The sample surfaces soaked in SBF for 15 days were analysed. The results indicate the absence of hydroxyapatite (HA) coating on the M and P group samples (Figs.6(a) and 6(b)). Meanwhile as shown in Fig.6(c), a significant amount of HA coating can be seen in the SEM image of the MN samples. Fig.6(d) shows the SEM image of the HA granule under a higher magnification.

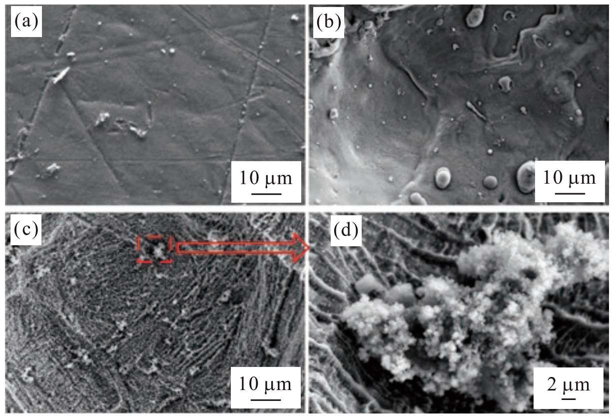

Fig.6 SEM images of samples soaked in SBF for 15 days with (a) polished, (b) micro pits, (c) and (d) micro/nano-textured surfaces

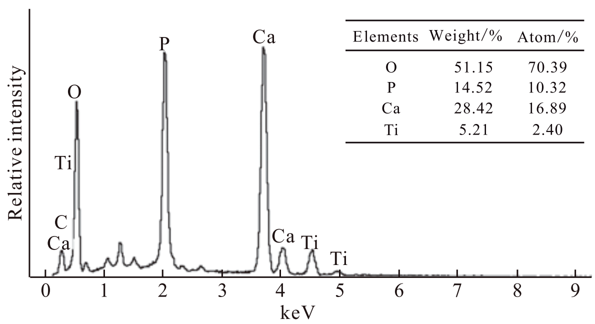

Elements	Weight/%	Atom/%
O	51.15	70.39
P	14.52	10.32
Ca	28.42	16.89
Ti	5.21	2.40

Fig.7 EDS profile of the HA granule

The porous particles shown in Figs.6(c) and 6(d) are similar to the morphology of HA. EDS analysis showed that the main elements of the HA granule were Ca, P, and O, as shown in Fig.7. The Ca/P atomic ratio was 1.636, which is close to the ratio in HA (1.6). Considering that the generation of other calcium phosphorus compounds and impurities is inevitable, the coating on the samples of group MN can be confirmed to be HA. In addition, the HA coating is thick and dense inside the micro pits, demonstrating that the micro pits are more conducive to the nucleation and growth of HA.

The multiscale micro/nano-texture in addition to increasing the specific surface area, was also beneficial to the aggregation of PO_4^{3-}, Ca^{2+}, OH^-, and HPO_4^{2-}, *etc*[31]. This increased the ionic concentration around the surface and when the calcium phosphate ion concentration in the microenvironment reached the nucleation threshold, an HA nucleus was generated on the samples. Once a stable nucleus forms, it absorbs various ions and grows, leading to the formation of a HA coating on the surface[32]. HA is usually composed of acicular, bar, or worm-like nanoparticles, as shown in Fig.6(d). The HA coating is thick and dense inside the submicron and nano pits because a three-dimensional morphology is beneficial to HA for its further growth and mechanical stability[33]. Further, the micro pits with a diameter of 150 μm and nanostructures with size in the range of 10-20 nm provide space for new bone tissue in-growth and osteoblast adhesion[34]. Therefore, the new proposed method to create multiscale micro/nano-textures on the Ti6Al4V surface is ideal for the bioactive modification of implants.

4 Conclusions

a)The effect of laser current on micro pits topography was analysed. Excessively low working current failed to generate micro-features on the surface and excessively large current caused serious surface ablation. The optimized working current was 13 A.

b)The clinkers generated by laser was cleaned completely by multiple acid etching. And submicron and nanoscale structures were superimposed on micro pits surface.

c)The multiscale micro/nano-textured surfaces with micro pits and submicron and nanoscale structures on the titanium alloy surface were obtained by laser treatment and acid etching. The diameter of the pits was about 150 μm and the depth was 50 μm. The submicron and nanoscale structures of 0.5-2 μm microgrooves and 10-20 nm nanopits were distributed on the micro pits surfaces.

d)There was thick and dense HA coating only observed on the multiscale micro/nano-textured surface compared with polished and micro-textured surface. This indicated that the multiscale micro/nano-texture surface showed better ability for HA formation, which increased the bioactivity of implants.

Acknowledgements

The authors would like to thank the Orthopaedic surgeons from Qilu Hospital, Shandong University, for provision of the technical help during experiment.

References

[1] Jarcho M, Kay JF, Gumaer KI, *et al.* Tissue, Cellular and Subcellular Events at a Bone-ceramic Hydroxylapatite Interface[J]. *Journal of Bioengineering*, 1977, 1(2): 79-92

[2] Barros RRM, Novaes JrAB, Papalexiou V, *et al.* Effect of Biofunctionalized Implant Surface on Osseointegration: a Histomorphometric Study in Dogs[J]. *Brazilian Dental Journal*, 2009, 20(2): 91-98

[3] Le Guéhennec L, Soueidan A, Layrolle P, *et al.* Surface Treatments of Titanium Dental Implants for Rapid Osseointegration[J]. *Dental Materials*, 2007, 23(7): 844-854

[4] Yang X, Zhang S, Jiang T. Bone Tissue Response to the Bone-like Tissue Coating on Titanium[J]. *Journal of Wuhan University of Technology-Mater. Sci. Ed.*, 2015, 30(1): 203-209

[5] Owen G R, Jackson J, Chehroudi B, *et al*. A PLGA Membrane Controlling Cell Behaviour for Promoting Tissue Regeneration[J]. *Biomaterials*, 2005, 26(35): 7 447-7 456

[6] Yang H, Zou H. Confocal Laser Scanning Microscope Evaluation of Early Bacterial Colonization on Zirconium Oxide and Titanium Surfaces: An in vivo Study[J]. *Journal of Wuhan University of Technology-Mater. Sci. Ed.*, 2013, 28(2): 396-399

[7] Sykaras N, Iacopino AM, Marker VA, *et al.* Implant Materials, Designs, and Surface Topographies: Their Effect on Osseointegration. A Literature Review[J]. *The International Journal of Oral & Maxillofacial Implants*, 1999, 15(5): 675-690

[8] Bormann KH, Gellrich NC, Kniha H, *et al*. Biomechanical Evaluation of a Microstructured Zirconia Implant by a Removal Torque Comparison with a Standard Ti-SLA Implant[J]. *Clinical Oral Implants Research*, 2012, 23(10): 1 210-1 216

[9] Liao H, Andersson AS, Sutherland D, *et al.* Response of Rat Osteoblast-like Cells to Microstructured Model Surfaces in Vitro[J]. *Biomaterials*, 2003, 24(4): 649-654

[10] Chappuis V, Buser R, Brägger U, *et al*. Long-Term Outcomes of Dental Implants with a Titanium Plasma-Sprayed Surface: A 20-Year Prospective Case Series Study in Partially Edentulous Patients[J]. *Clinical Implant Dentistry and Related Research*, 2013, 15(6): 780-790

[11] Tang B, Lin N, Li X, *et al.* Bacteria Adherence Properties of Nitrogen-doped TiO_2 Coatings by Plasma Surface Alloying Technique[J]. *Journal of Wuhan University of Technology-Mater. Sci. Ed.*, 2012, 27(3): 542-546

[12] Yoshida Y, Kuroda K, Ichino R, *et al.* Influence of Surface Properties on Bioactivity and Pull-out Torque in Cold Thread Rolled Ti Rod-Development of Bioactive Metal-forming Technology[J]. *CIRP Annals-Manufacturing Technology*, 2012, 61(1): 579-582

[13] Webster TJ, Ejiofor JU. Increased Osteoblast Adhesion on Nanophase Metals: Ti, Ti6Al4V, and CoCrMo[J]. *Biomaterials*, 2004, 25(19): 4 731-4 739

[14] Chen R, Zheng J, Nie P, *et al*. Two-step Anodization of Maltilayer TiO_2 Nanotube and Its Photocatalytic Activity under UV Light[J]. *Journal of Wuhan University of Technology-Mater. Sci. Ed*., 2012, 27(5): 866-870

[15] Frank MJ, Walter MS, Lyngstadaas SP, *et al*. Hydrogen Content in Titanium and a Titanium-zirconium Alloy After Acid Etching[J]. *Materials Science and Engineering C*, 2013, 33(3): 1 282-1 288

[16] Vorobyev AY, Guo C. Femtosecond Laser Structuring of Titanium Implants[J]. *Applied surface science*, 2007, 253(17): 7 272-7 280

[17] Reimers H, Gold J, Kasemo B, *et al*. Topographical and Surface Chemical Characterization of Nanosecond Pulsed-laser Micromachining of Titanium at 532-nm Wavelength[J]. *Applied Physics A*, 2003, 77(3-4): 491-498

[18] Reddy S, Wasnik S, Guha A, *et al*. Evaluation of Nano-biphasic Calcium Phosphate Ceramics for Bone Tissue Engineering Applications: in vitro and Preliminary in vivo Studies[J]. *Journal of Biomaterials Applications*, 2013, 27(5): 565-575

[19] Ho YH, Vora HD, Dahotre NB. Laser Surface Modification of AZ31B Mg Alloy for Bio-wettability[J]. *Journal of Biomaterials Applications*, 2015, 29(7): 915-928

[20] Kurella A, Dahotre NB. Review Paper: Surface Modification for Bioimplants: the Role of Laser Surface Engineering[J]. *Journal of Biomaterials Applications*, 2005, 20(1): 5-50

[21] Mendonça G, Mendonça DBS, Aragao FJL, *et al*. Advancing Dental Implant Surface Technology-from Micron-to Nanotopography[J]. *Biomaterials*, 2008, 29(28): 3 822-3 835

[22] Buser D, Broggini N, Wieland M, *et al*. Enhanced Bone Apposition to a Chemically Modified SLA Titanium Surface[J]. *Journal of Dental Research*, 2004, 83(7): 529-533

[23] Ellingsen JE, Johansson CB, Wennerberg A, *et al*. Improved Retention and Bone-tolmplant Contact with Fluoride-modified Titanium Implants[J]. *The International Journal of Oral and Maxillofacial Implants*, 2003, 19(5): 659-666

[24] Liu H, Webster TJ. Mechanical Properties of Dispersed Ceramic Nanoparticles in Polymer Composites for Orthopedic Applications[J]. *International Journal of Nanomedicine*, 2010, 5: 299-313

[25] Yao C, Slamovich EB, Webster TJ. Enhanced Osteoblast Functions on Anodized Titanium with Nanotube-like Structures[J]. *Journal of Biomedical Materials Research Part A*, 2008, 85(1): 157-166

[26] Mendonca G, Mendonça DBS, Simoes L G P, *et al.* The Effects of Implant Surface Nanoscale Features on Osteoblast-specific Gene Expression[J]. *Biomaterials*, 2009, 30(25): 4 053-4 062

[27] Aparicio C, Padrós A, Gil FJ. In Vivo Evaluation of Micro-rough and Bioactive Titanium Dental Implants Using Histometry and Pull-out Tests[J]. Journal of the Mechanical Behavior of Biomedical Materials, 2011, 4(8): 1 672-1 682

[28] Hallab NJ, Vermes C, Messina C, *et al.* Concentration-and Composition-dependent Effects of Metal Ions on Human MG-63 Osteoblasts[J]. *Journal of Biomedical Materials Research*, 2002, 60(3): 420-433

[29] Tengvall P, Lundström I, Sjöqvist L, *et al.* Titanium-hydrogen Peroxide Interaction: Model Studies of the Influence of the Inflammatory Response on Titanium Implants[J]. *Biomaterials*, 1989, 10(3): 166-175

[30] Li P, Ohtsuki C, Kokubo T, *et al*. The Role of Hydrated Silica, Titania, and Alumina in Inducing Apatite on Implants[J]. *Journal of Biomedical Materials Research*, 1994, 28(1): 7-15

[31] Oh S H, Finones RR, Daraio C, *et al*. Growth of nano-scale Hydroxyapatite Using Chemically Treated Titanium Oxide Nanotubes[J]. *Biomaterials*, 2005, 26(24): 4 938-4 943

[32] Dong LM, Wang C. Study on the Structure Analysis and Forming Mechanism of Bone-like Apatite. Journal of Functional Materials 2004, 35:2397-2400 (Chinese)

[33] Barrere F, Snel MME, van Blitterswijk C A, *et al*. Nano-scale Study of the Nucleation and Growth of Calcium Phosphate Coating on Titanium Implants[J]. *Biomaterials*, 2004, 25(14): 2 901-2 910

[34] Jonášová L, Müller FA, Helebrant A, *et al*. Biomimetic Apatite Formation on Chemically Treated Titanium[J]. *Biomaterials*, 2004, 25(7): 1 187-1 194